Food Hydrocolloids 162 (2025) 111011

Contents lists available at ScienceDirect

Food Hydrocolloids

journal homepage: www.elsevier.com/locate/foodhyd

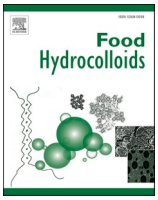

# Influence of structural properties of textured vegetable proteins on *in vitro* gastric digestion kinetics of plant-based meat analogue patties

Dan Liu [a,*], Thiemo van Esbroeck [b], Anja E.M. Janssen [c], Elke Scholten [b], Paul A.M. Smeets [a], Markus Stieger [a]

[a] Division of Human Nutrition & Health, Wageningen University & Research, Wageningen, the Netherlands
[b] Physics and Physical Chemistry of Foods, Wageningen University & Research, Wageningen, the Netherlands
[c] Laboratory of Food Process Engineering, Wageningen University & Research, Wageningen, the Netherlands

ARTICLE INFO

*Keywords:*
Plant-based patties
Textured vegetable proteins
Microstructure
Macrostructure
Protein digestion

ABSTRACT

Textured vegetable proteins (TVPs) differ in structural properties that may affect the protein digestion of TVP-based meat analogues. This study explored the influence of structural properties on *in vitro* gastric protein digestion of TVPs and TVP-based patties. Eight TVPs differing in macroscopic surface area and microstructural properties (porosity, wall density, etc.) were used. As references, TVPs were ground into powders to remove their porous structure. *In vitro* gastric protein digestion was determined following the INFOGEST protocol. Structural properties were correlated with free amino group concentrations at different digestion times. For intact TVPs, surface area ($r = 0.78$) and mean pore size ($r = 0.74$) showed significant positive correlations with free amino group concentrations at 5 min of digestion. These correlations persisted for patties (at 30–120 min for surface area, 5–60 min for mean pore size). For TVP powders, wall density was the main structural feature, which was negatively correlated with free amino group concentrations at 5 min ($r = -0.78$) and 30 min ($r = -0.91$) of digestion. Wall density was not correlated with protein digestion for intact TVPs and patties. We conclude that pore-related rather than wall-related TVP properties dominated protein digestion of TVPs and patties. Larger macroscopic surface area and larger mean pore size contributed more to accelerating protein hydrolysis during digestion of TVPs and TVP-based patties than smaller wall density. These results suggest that altering TVP microstructure could potentially be a way to enhance protein digestibility of plant-based meat analogues.

## 1. Introduction

Sufficient protein intake in the daily diet is important to maintain and promote human health. Proteins in foods undergo a complex digestion process and are eventually absorbed as free amino acids, which are crucial for protein synthesis and other metabolic processes (Capuano & Janssen, 2021). Nowadays, conventional animal-based proteins are increasingly being replaced by proteins from other sources, especially plants, due to their contribution to greenhouse gas emissions, land and water use, and environmental pollution. Plant-based meat analogues have been developed, with the aim to mimic the texture and flavor of meat or meat products (Baune, Terjung, Tülbek, & Boukid, 2022; Imran & Liyan, 2023), which contributes to the transition towards plant-based dietary patterns. However, plant-based proteins are known to have lower protein quality and digestibility compared to animal-based proteins, due to their unbalanced amino acid profile and the presence of antinutritional factors (Gorissen et al., 2018; Kaur et al., 2022; Sá, Moreno, & Carciofi, 2020; Xie et al., 2022). Understanding and improving protein digestibility recently gained more attention as a result of the development of plant-based meat analogues (Sá et al., 2020).

Following the macroscopic breakdown of solid foods during the oral phase, food boli pass through the esophagus into the stomach, where the enzymatic digestion of proteins begins. In the stomach, the acidic gastric environment facilitates the hydrolysis of peptide bonds by pepsins, initiating the breakdown of proteins. Subsequent digestion in the small intestine involves further enzymatic action, with trypsin and chymotrypsin catalyzing the breakdown of polypeptides into smaller peptides and free amino acids, which are then available for absorption (Capuano & Janssen, 2021; Kong & Singh, 2008). Gastric protein digestion is influenced by food micro- and macrostructure (Liu, Janssen, Smeets, & Stieger, 2024, Liu et al., 2024; Barbé et al., 2013; Zhang et al., 2023;

* Corresponding author.
*E-mail address:* dan1.liu@wur.nl (D. Liu).

https://doi.org/10.1016/j.foodhyd.2024.111011
Received 13 September 2024; Received in revised form 20 December 2024; Accepted 21 December 2024
Available online 24 December 2024

Zhao, Wu, Chen, Zhao, & Sun, 2020). For example, Zhang et al. (2023) showed that the loose and fragmentary microstructure of myofibrillar protein gels was strengthened by the addition of carboxymethylated cellulose nanofibrils, forming a denser and porous structure. Both the denser structure and harder texture contributed to the decrease in *in vitro* gastric protein hydrolysis (Zhang et al., 2023). Similar results were observed in soy protein gels. *In vitro* gastric digestion was hindered by modifying the gel microstructure from a coarse and loose structure to a dense ordered porous structure (Zhao et al., 2020). We reported previously that whey protein isolate/polysaccharides mixed gels with similar macrostructures and mechanical properties but differing in microstructure showed differences in protein digestion (Liu et al., 2024). Mixed gels with a homogeneous microstructure showed a less aggregated protein network, facilitating the proteolysis during *in vitro* gastric protein digestion, whereas gels with a heterogeneous microstructure with an aggregated protein phase showed slower protein digestion (Liu et al., 2024). At macroscopic length scales, larger total surface area typically resulted in more protein hydrolysis during *in vitro* gastric digestion (Liu et al., 2024; Mennah-Govela & Bornhorst, 2021). Large whey protein gel cubes, with a small total surface area, showed lower degree of protein hydrolysis after the *in vitro* gastric digestion than small gel cubes, with a larger total surface area (Mennah-Govela & Bornhorst, 2021). Moreover, the impact of surface area on protein digestion interacts with gel microstructure. After a 2.6-fold increase in total surface area of whey protein gels, the *in vitro* gastric protein digestion rate increased the most in gels with a bi-continuous microstructure (2.5-fold) followed by gels with protein continuous (2.0-fold), coarse stranded (1.8-fold) and homogeneous (1.8-fold) microstructure (Liu et al., 2024). These studies on colloidal systems demonstrated role of micro- and macrostructure in *in vitro* gastric protein digestion.

Such differences in micro- and macrostructural properties are also present in textured vegetable proteins (TVPs), which provide meat-like texture in plant-based meat analogues (Baune et al., 2022; van Esbroeck, Sala, Stieger, & Scholten, 2024). Extrusion technology is commonly used to produce TVPs (Baune et al., 2022). The shape, particle size, and structural properties, such as porosity, of TVPs can be varied by adjusting the composition and extrusion conditions during production (Brishti et al., 2021; Flory & Alavi, 2024; Jeon, Gu, & Ryu, 2023; Samard, Gu, & Ryu, 2019; Samard, Maung, Gu, Kim, & Ryu, 2021). The structure of TVPs strongly influences their functional properties and those of TVP-based meat analogues (Flory & Alavi, 2024; Samard et al., 2021; van Esbroeck et al., 2024). van Esbroeck et al. (2024) characterized the microstructural properties (porosity, mean pore size, mean wall thickness, wall density, apparent density, absolute density, density-based porosity) water absorption capacity (WAC) and water holding capacity (WHC) of 13 commercial TVPs. They found that porosity was positively correlated with the maximum water absorption capacity and the water holding capacity of TVPs (van Esbroeck et al., 2024). In another study, TVPs with a compact structure and smaller internal pores showed higher bulk density and lower water holding capacity (Flory & Alavi, 2024). These studies reported the impact of TVP structure on rehydration properties, which has been related to the functional and sensory properties of TVP-based patties (Hong, Shen, & Li, 2022; Samard et al., 2021; van Esbroeck et al., 2024). Therefore, TVP structure is a crucial factor to consider when developing TVP-based meat analogues.

Although numerous studies have explored the structural properties of TVPs and functional properties of TVP-based patties, the nutritional quality of TVP-based meat analogues remains underexplored (Ishaq, Irfan, Sameen, & Khalid, 2022). A few studies suggested that the structure of TVPs may affect protein digestion (Azzollini, Derossi, Fogliano, Lakemond, & Severini, 2018; Lin et al., 2022; Wang et al., 2024). Wang et al. (2024) recently reported that the structure of low moisture TVPs made from soybean and/or pea protein influenced *in vitro* protein digestibility. TVPs made from a 1 : 1 mixture of soybean and pea protein showed a denser and more compact structure. These TVPs had lower free amino acid concentrations in digesta compared to TVPs made from soybean protein concentrate, which showed a loose and porous structure (Wang et al., 2024). Also the ratio of pore wall thickness to pore size has been shown to be negatively correlated with the *in vitro* protein digestibility for extruded wheat snacks enriched with mealworm powder (Azzollini et al., 2018). For textured wheat protein, the loose, fiber-like structure with large gaps was shown to contribute to higher *in vitro* protein digestibility, although this structure-driven impact could be neutralized by changes in protein molecular interactions after the addition of sodium tripolyphosphate (Lin et al., 2022, 2023). These studies demonstrate that the microstructure of TVPs influences *in vitro* protein digestion of TVPs. Most of these studies used qualitative visual comparisons of microstructure images to characterize the microstructural properties of the TVPs, rather than employing quantitative image analysis to characterize different structural features, such as surface area, porosity, pore size, wall thickness, and wall density. Consequently, there is limited quantitative information available on the relationships between structural properties of TVPs (e.g., pore size and wall density) and protein digestion of TVPs. Moreover, the studies above investigated the impact of TVP structure on the digestion of TVP itself, which typically needs to be mixed with other ingredients to make meat analogue products and cooked before being consumed and digested. The impact of structural properties of TVPs on the digestion of TVP-based products is not known yet. The interaction between TVPs and other ingredients, as well as the cooking process might affect the protein digestibility of TVP-based meat analogues. A thorough understanding of the impact of TVP structure on protein digestion of TVP-based meat analogues may provide valuable insights for improving the protein digestibility of plant-based meat analogues, benefiting the development of nutritious plant-based protein foods.

This study aims to explore the impact of structural properties (surface area, porosity, mean pore size, mean wall thickness, wall density, apparent density, absolute density, density-based porosity), water absorption and acid absorption of TVPs on the *in vitro* gastric protein digestion of TVPs and TVP-based patties. Eight commercial TVPs differing in structural properties from two protein sources (yellow pea and soybean) were used. The surface area reported in this study refers to the macroscopic surface area of TVPs. Porosity, mean pore size, mean wall thickness, wall density, apparent density, absolute density, density-based porosity represent the microscopic structural properties. As a control, TVPs were ground into fine powders to eliminate the porous structure of TVPs. We hypothesize that a) surface area, porosity, mean pore size, density-based porosity, water absorption capacity and acid absorption positively correlate with protein hydrolysis during *in vitro* gastric digestion of intact TVPs and TVP-based patties and b) mean wall thickness, wall density, apparent density and absolute density negatively correlate with protein hydrolysis during the *in vitro* gastric digestion of intact TVPs and TVP-based patties.

## 2. Materials and methods

### 2.1. Materials

Eight commercially available textured vegetable proteins (TVP) from three suppliers were used. Pea protein TVPs were obtained from Roquette Frères S.A (Lestrem, France). Soy granules (Soja Granulat) and soy strips (Soja Geschnetzeltes) were obtained from Vegafit (Deventer, The Netherlands). Soy Flakes and Soy Chunks XL from the VITATEX® range were kindly provided by GoodMills Innovation GmbH (Hamburg, Germany). The commercial name, supplier, sample code, source, and protein content are summarized in Supplementary Table 1. Methylcellulose (MC, viscosity at 2%: 4000 mPas) was purchased from Sigma Aldrich (St. Louis, MO, USA). Pea protein isolate (PPI) (NUTRALYS® F85M) was obtained from Roquette Frères S.A., (Lestrem, France). Sunflower oil (Reddy, Vandemoortele Nederland BV, Zeewolde, The Netherlands) and sodium chloride were purchased from a local

supermarket (Jumbo, Veghel, The Netherlands). Pepsin from porcine gastric mucosa and other chemicals were purchased from Sigma-Aldrich (St. Louis, USA).

### 2.2. Characterization of the structure properties of TVPs

The structural characteristics of TVP pieces have been previously reported by van Esbroeck et al. (2024). In short, porosity, mean pore size, mean wall thickness and wall density were analyzed using X-ray microtomography (XRT) and image analysis (van Esbroeck et al., 2024). The apparent density, absolute density and density-based porosity were determined using a displacement method. These methods and the results of the characterization have been described in detail by van Esbroeck et al. (2024). The structural characteristics (porosity, mean pore size, mean wall thickness, wall density, apparent density, absolute density, density-based porosity) of the eight commercial TVPs used in this study (ROQ1, ROQ2, ROQ3, ROQ5, VEG1, VEG2, GIM1 and GMI2) are summarized in Table 1 and discussed briefly in section 3.1.1.

### 2.3. Sample preparation

Each TVP sample was prepared in three forms: powder, intact TVP and patty. Dry TVP particles were blended in a Thermomix (TM5, Vorwerk & Co. KG, Wuppertal, Germany) at high speed followed by sieving with a 2 mm sieve to obtain fine powders. The rationale for blending the dry TVP particles into powders was to remove macroscopic structural characteristics of the TVPs. Powders were rehydrated in water (TVP: water ratio of 1:2 based on weight) for 30 min and stirred every 10 min (VEG2 was rehydrated with 1.5 times its weight). Intact TVPs were rehydrated following the same process as the powders. For samples ROQ1, ROQ5, VEG1 and GMI1, rehydrated TVPs were ready for further analysis. For samples ROQ2, ROQ3, VEG2 and GMI2, rehydrated TVPs were blended in a Thermomix at a speed of 5 for 20 s to slightly reduce their size while maintaining their initial structure. Plant-based meat analogue patties were prepared from the rehydrated TVPs (60 w/w%), sun flower oil (15 w/w%), pea protein isolate (5 w/w%), methylcellulose (2 w/w%), NaCl (0.8 w/w%) and water (17.2 w/w%) following the process described previously by van Esbroeck et al. (2024). Briefly, rehydrated TVPs were first mixed with all dry ingredients for 1 min. Water was then added to the ingredients and mixed for 1 min followed by the addition of oil and mixing for 1 min. The patty batter was mixed for an additional minute and stored in a fridge overnight (4 °C). The patty batter was shaped into patties of 100 g using a patty shaper (diameter 70 mm; thickness 20 mm). The patties were placed individually in plastic cooking bags from which air was removed and cooked for 1 h at 70 °C in a water bath. After cooling down to room temperature, the patties were cut into pieces and the TVP particles were gently separated with a spatula. All samples were freshly prepared and subjected to further analysis within 12 h.

### 2.4. Sample characterization

#### 2.4.1. Surface area of TVP powder

Dynamic Vapour Sorption was used to determine the specific surface area of TVP powders (Young, Edge, Staniforth, Steele, & Price, 2005). Dry powder (5–10 mg) was placed in a hemispherical metal-coated quartz pan and loaded into a Discovery SA Dynamic Vapour Sorption (DVS) Analyser (TA instruments, New Castle, DA, USA). The Relative Humidity (RH) of the chamber was decreased to 0% within 60 min. Then, the RH was increased from 10% to 90% in 9 steps at constant temperature of 20 °C. The criterion for increasing humidity was a weight change of the sample of less than 0.1% for 60 min. The sorption isotherm data were analyzed using TRIOS Software v5.6 (TA instruments, New Castle, DA, USA). The relative sample weight (%) was plotted against the RH. GAB analysis was applied over the range of 10–90% RH to determine the specific surface area ($m^2/g$). Measurements were performed in duplicate.

#### 2.4.2. Surface area of rehydrated TVPs and patties

Two-dimensional image analysis was used to estimate the macroscopic surface area of rehydrated TVPs and patties (Chen, Capuano, & Stieger, 2021). A small amount of sample weighing 1.3–3.0 g was placed in a petri dish (120 × 120 × 17 mm) and pieces were manually separated using a spatula. The dishes were scanned individually on a flatbed scanner (Canon CanoScan 9000 F MarkII) to capture high-resolution color images at 600 dpi against a black background. The captured images were analyzed using ImageJ software (version 1.52a, National Institutes of Health). The images were converted to 8-bit followed by adjusting the brightness/contrast and black/white threshold to generate binary images. The "Analyze Particles" function in ImageJ was used to quantify the surface area ($mm^2$) of each particle from a top view. The total surface area was then summed and normalized by the sample weight, providing the specific surface area ($mm^2/g$) of rehydrated TVPs or particles separated from the patty. To reduce noise, particles smaller than the smallest visible particles among each sample or with a circularity below specific levels depending on the particle shape were excluded (Supplementary Table 2). Two measurements were taken for each petri dish and averaged. For each sample, five replicates were taken, and the results were averaged.

#### 2.4.3. Water absorption capacity of rehydrated TVPs at pH 2

The water absorption capacity of rehydrated TVPs at pH 2 in simulated gastric fluid (SGF) was determined in duplicate using the method described by van Esbroeck et al. (2024) with modifications. Approximately 20 g of rehydrated TVPs was submerged in 500 mL SGF (containing 25 mmol/L $NaHCO_3$ and 47.2 mmol/L NaCl, pH = 2). At time 1, 2, 5, 10, and 20 min, the sample was poured through a sieve with a 2 mm mesh, drained and the obtained TVP was weighed, after which it was put back into the SGF. After 30 min, the samples was again poured through the sieve, after which the TVPs were drained and weighed without putting them back in the SGF. Around 90 g of remaining SGF was

**Table 1**
Characteristics of eight commercial TVPs: XRT-based porosity ($\Phi_{XRT}$), mean pore size (MPS), mean wall thickness (MWT), wall density ($\rho_{wall}$) as obtained from XRT measurements; apparent density ($\rho_{app}$), absolute density ($\rho_{abs}$) and density-based porosity ($\Phi_{density}$) from density measurements. Means are reported with standard deviation. Means sharing superscript letters are not significantly different ($p > 0.05$). Table is adapted from van Esbroeck et al. (2024).

| TVP type | XRT | | | | Density measurements | | |
|---|---|---|---|---|---|---|---|
| | $\Phi_{XRT}$ (%) | MPS (μm) | MWT (μm) | $\rho_{wall}$ ($kg{\cdot}m^{-3}$) | $\rho_{app}$ ($kg{\cdot}m^{-3}$) | $\rho_{abs}$ ($kg{\cdot}m^{-3}$) | $\Phi_{density}$ (%) |
| ROQ1 | $63.8 \pm 11.6^{cd}$ | $526 \pm 138^{ab}$ | $239 \pm 5^{abc}$ | $1379 \pm 462^{c}$ | $500 \pm 51^{def}$ | $1303 \pm 4^{b}$ | $60.3 \pm 3.9^{bcd}$ |
| ROQ2 | $80.9 \pm 1.9^{d}$ | $1921 \pm 661^{c}$ | $196 \pm 64^{ab}$ | $1298 \pm 139^{abc}$ | $248 \pm 8^{a}$ | $1298 \pm 1^{b}$ | $78.0 \pm 0.6^{ef}$ |
| ROQ3 | $65.7 \pm 20.8^{cd}$ | $3152 \pm 1135^{bc}$ | $108 \pm 9^{a}$ | $597 \pm 362^{a}$ | $205 \pm 8^{a}$ | $1294 \pm 4^{b}$ | $81.4 \pm 0.7^{f}$ |
| ROQ5 | $57.7 \pm 3.0^{bcd}$ | $559 \pm 77^{ab}$ | $266 \pm 26^{abc}$ | $1036 \pm 186^{abc}$ | $438 \pm 72^{bcde}$ | $1307 \pm 7^{b}$ | $65.8 \pm 5.5^{bcdef}$ |
| VEG1 | $27.1 \pm 1.4^{a}$ | $251 \pm 257^{a}$ | $287 \pm 7^{de}$ | $1429 \pm 159^{c}$ | $1042 \pm 114^{g}$ | $1364 \pm 3^{d}$ | $22.8 \pm 8.4^{a}$ |
| VEG2 | $32.0 \pm 4.7^{a}$ | $2817 \pm 629^{d}$ | $657 \pm 104^{f}$ | $1515 \pm 113^{c}$ | $1031 \pm 30^{g}$ | $1375 \pm 3^{d}$ | $24.0 \pm 2.2^{a}$ |
| GMI1 | $39.8 \pm 2.9^{ab}$ | $554 \pm 82^{ab}$ | $219 \pm 15^{abcd}$ | $973 \pm 91^{abc}$ | $586 \pm 47^{ef}$ | $1406 \pm 9^{e}$ | $58.4 \pm 3.4^{bc}$ |
| GMI2 | $64.9 \pm 1.7^{cd}$ | $4790 \pm 1726^{d}$ | $220 \pm 6^{abcd}$ | $888 \pm 201^{abc}$ | $312 \pm 69^{abc}$ | $1380 \pm 1^{d}$ | $77.9 \pm 5.0^{ef}$ |

transferred to a tray and dried in an oven (Binder MDL 115, Keison products, Chelmsford, UK) at 105 °C to obtain the sample loss on dry matter during the measurement. The initial mass of the sample was corrected by the sample loss and dry matter content of rehydrated TVPs using:

$$corrected\ m_0 = m_0 - \frac{\frac{m_{(after)} \times m_{(SGF)}}{m_{(before)}}}{\text{dry matter content of rehydrated TVPs}} \quad (1)$$

where $m_0$ is the initial measured mass of sample; $m_{(before)}$ is the weight of SGF before drying; $m_{(after)}$ is the weight of dry matter of the SGF after drying; $m_{(SGF)}$ is the total mass of SGF after 30-min test; dry matter content of rehydrated TVPs is 33% (40% for VEG2).

The water absorption (WA) of rehydrated TVPs at pH 2 was calculated as:

$$WA\ (\%) = \frac{m_{(t)} - corrected\ m_0}{corrected\ m_0} \times 100 \quad (2)$$

where $m_{(t)}$ is the measured mass of samples at certain time point. The water absorption capacity (WAC) is defined as the water absorption after 30 min.

### 2.5. In vitro gastric protein digestion of rehydrated TVP powders, rehydrated intact TVPs and patties

The *in vitro* gastric protein digestion was performed following the INFOGEST 2.0 protocol with minor modifications (Brodkorb et al., 2019). The oral phase of digestion (dilution of food with simulated salivary fluid and simulated mastication) was omitted in this study. The oral phase of digestion was omitted because the structural properties (porosity, mean pore size, mean wall thickness, wall density, apparent density, absolute density, density-based porosity) of eight commercial TVPs were characterized in a previous study (van Esbroeck et al., 2024). The macroscopic structural breakdown during mastication would have changed these previously determined initial structural properties of the TVPs. This study focused on correlating the (initial) structural properties of TVPs with their *in vitro* gastric protein hydrolysis quantified by the free amino group concentration in the gastric juice. Three grams of rehydrated TVP powder, rehydrated TVP or patties were immersed in 30 mL of SGF (containing 25 mmol/L $NaHCO_3$, 47.2 mmol/L NaCl and 2000 U/mL pepsin, pH = 2) for 2 h at 37 °C under continuous gentle stirring. The pH of gastric juice was kept constant at 2 by titrating with a 1 M HCl solution using an automated titrator. The amount of added acid was recorded over time to represent acid consumption (mmol) during digestion. Small amounts (100 μL) of liquid were taken at time 5, 30, 60 and 120 min followed by dilution with SGF without pepsin. The diluted mixtures were heated at 90 °C for 5 min while mixing to deactivate pepsin. After cooling down to room temperature, samples were stored at 4–5 °C for further analysis. This digestion experiment was performed in triplicate.

The o-phthaldialdehyde (OPA) method (Nielsen, Petersen, & Dambmann, 2001) was applied to quantify the free amino group concentration in gastric juice over time. Briefly, the mixtures of 10 μL sample solution and 200 μL OPA reagent in 96-plate wells were shaken for 3 min in a microplate photometer (Thermo Scientific 357, USA). The absorption of mixed solutions at 340 nm was determined immediately after shaking. A calibration curve made with serine standard solutions (0–200 mg/mL) was used to convert the absorption values to free amino group concentrations.

Additionally, all samples were subjected to *in vitro* gastric protein digestion as described above but in the absence of pepsin (blank digestion), in order to detect the free amino groups present in SGF while only incubating samples under *in vitro* gastric digestion condition. The free amino group concentration in SGF during blank digestion was determined at 0, 5, 30, 60 and 120 min. The amount of added acid during blank digestion was monitored to represent the acid absorption (mmol) of samples under *in vitro* gastric protein digestion condition. The blank digestion was performed in triplicate.

The free amino group concentration in gastric juice at each time point during digestion was corrected:

$$\text{free amino group concentration} = Mean_{(digestion)} - Mean_{(blank\ digestion)} \quad (3)$$

where $Mean_{(digestion)}$ refers to the average of the free amino group concentration measured during digestion at the corresponding time point (in triplicate); $Mean_{(blank\ digestion)}$ refers to the average of the free amino group concentration measured during blank digestion (in absence of pepsin) at the corresponding time point (in triplicate).

### 2.6. Data analysis

The data of surface area, WAC at pH 2, acid consumption during digestion and acid absorption in absence of pepsin were analyzed using one-way analysis of variance (ANOVA) followed by a Tukey's HSD post-hoc test using SPSS statistics software (IBM SPSS Statistics Version 28, IBM Corp). Statistical significance was determined at a threshold of $p = 0.05$. Results are presented as means with standard deviations (SD). The standard deviations of free amino group concentration were calculated as:

$$SD = \sqrt{\sigma^2_{(digesion)} + \sigma^2_{(blank\ digesion)}} \quad (4)$$

where $\sigma^2_{(digesion)}$ refers to the SD of free amino group concentrations measured during digestion; the $\sigma^2_{(blank\ digesion)}$ refers to the SD of free amino group concentrations measured during blank digestion.

Two-tailed Pearson correlation analysis was performed using SPSS statistics software (IBM SPSS Statistics Version 28, IBM Corp) based on mean values to obtain the correlation coefficients between the structural properties of TVPs (surface area, porosity, mean pore size, mean wall thickness, wall density, apparent density, absolute density, density-based porosity WAC, WAC at pH 2, acid consumption during digestion, acid absorption in absence of pepsin) and free amino group concentrations at each time point. Scatter plots of free amino group concentration during digestion against sample characteristics and linear regressions were obtained by running a Python code in Visual Studio Code (Microsoft Corp.)

## 3. Results and discussion

### 3.1. Sample characterization

#### 3.1.1. Structural properties of TVPs

The two-dimensional image slices of the microstructure of the eight TVPs are shown in Supplementary Fig. 1 (images are reproduced from van Esbroeck et al., 2024). Table 1 summarizes the structural features (porosity, mean pore size, mean wall thickness, wall density, apparent density, absolute density, density-based porosity) of the eight TVPs (reproduced from van Esbroeck et al., 2024). The porosity of TVPs determined by XRT ranged from 27 to 81%, mean pore size from 251 to 4790 μm, mean wall thickness from 108 to 657 μm, wall density from 597 to 1515 $kg{\cdot}m^{-3}$, and apparent density from 205 to 1042 $kg{\cdot}m^{-3}$ showing that the TVPs differed substantially in structural features. This can be attributed to the properties of the raw materials and the different extrusion conditions resulting in different expansion ratios and consequently different structures. For some TVPs (ROQ3, GMI1 and GMI2), the XRT-based porosity and density-based porosity deviated considerably from each other, which was related to the wall density of the TVP (van Esbroeck et al., 2024). Pores smaller than 15 μm were not identified and therefore not included in the determination of XRT-based porosity due to the spatial resolution (15 μm) of the XRT measurements. TVPs where XRT-based porosity and density-based porosity are very similar

have a negligible amount of pores smaller than 15 μm.

### 3.1.2. Surface area, water absorption and acid absorption of rehydrated TVP powders, rehydrated intact TVPs and patties

For all samples, the surface area of powders was more than four orders of magnitude larger than that of intact TVPs and patties (Table 2). The surface area of intact TVPs and patties ranged from 558 to 1740 $mm^2/g$ and 561–1226 $mm^2/g$, respectively, whereas the surface area of the TVP powders ranged from 164 to 231 $m^2/g$. The water absorption of rehydrated intact TVPs at pH 2 was given at 30 min of incubation (Table 2), even though it barely changed anymore after the first minute (Supplementary Fig. 2). The WAC of dry TVPs at neutral pH reported by van Esbroeck et al. (2024) is also provided. As expected, the WAC of rehydrated TVPs at pH 2 was lower than that of dry TVPs due to their higher water content.

The acid absorption of samples in SGF without pepsin is shown in Table 2 and Supplementary Fig. 3. The acid absorption of rehydrated TVP powders occurred rapidly during the first 5 min and then leveled off at 1.10–1.40 mmol. Compared to TVP powders, the acid absorption of intact TVPs was slower (Supplementary Fig. 3). After 5 min, the acid absorption of intact TVPs ranged from 0.60 to 1.18 mmol and increased to 1.14–1.52 mmol after 120 min. The slower acid absorption of intact TVPs can be attributed to the presence of a porous structure and the much smaller surface area than powders. After 120 min, patties showed less acid absorption than the corresponding powders and intact TVPs (Table 2). This might be ascribed to the addition of other ingredients to the patty, such as methylcellulose, which might fill the pores in TVPs, and thereby inhibit acid diffusion (Zuo et al., 2024).

## 3.2. In vitro gastric protein digestion of rehydrated TVP powders, rehydrated intact TVPs and TVP patties

The free amino group concentrations in SGF during *in vitro* gastric protein digestion of rehydrated TVP powders, rehydrated intact TVPs and TVP patties are shown in Fig. 1. Generally, TVP powders showed higher free amino group concentrations during the first 30 min of *in vitro* gastric protein digestion than intact TVPs and patties, indicating a faster protein hydrolysis at the beginning of digestion for powders compared to TVPs and patties. This was attributed to the much larger surface area (four orders of magnitude) of TVP powders compared to that of TVPs and patties (Table 2).

The eight samples were divided into two groups depending on protein source to allow for comparison of the effect of structure on protein hydrolysis independent of protein type. Fig. 1a–c represent results for yellow pea protein, whereas Fig. 1d–f shows results for soy protein. For yellow pea, the powders of ROQ2, ROQ3 and ROQ5 displayed similar free amino group concentrations during digestion, while ROQ1 showed the lowest free amino group concentrations (Fig. 1a). Similar trends were observed for the intact TVPs (Fig. 1b), although the differences between ROQ1 and other samples were larger. Surprisingly, differences in protein hydrolysis among ROQ2, ROQ3 and ROQ5 were observed in patties, where ROQ3 showed the highest free amino group concentrations during digestion (Fig. 1c). For soybean samples, GMI1 and GMI2 powders exhibited similar free amino group concentrations during digestion, as did VEG1 and VEG2 except at 60 min. Generally, GMI powders had higher free amino group concentrations than VEG powders (Fig. 1d). Such a trend was not displayed for the intact rehydrated TVPs, as GMI1 showed the lowest free amino group concentrations instead of the VEG samples, although GMI2 still showed the highest concentrations. VEG1 and VEG2 still displayed a similar evolution of the free amino group concentrations (Fig. 1e). For patties, the four curves became more separated than the curves of TVP powders and intact TVPs (Fig. 1f). Specifically, the difference between GMI1 and GMI2 observed for intact TVPs was sustained for patties. Unlike powders and TVPs, VEG2 patties exhibited clearly higher free amino group concentrations than VEG1 patties.

The observed differences in protein digestion between TVP powders of the same protein source could be attributed to various reasons, such as differences in composition or extrusion processing techniques applied by different producers (e.g., VEGs and GMIs). It is reported that the digestibility of plant proteins can be affected by fractionation methods, processing conditions and interactions with other components (Del Rio, Boom, & Janssen, 2022; Sá et al., 2020). Additionally, differences in wall density between TVP powders (van Esbroeck et al., 2024) potentially affected the protein digestion of powders. For TVPs and patties, the differences in protein hydrolysis could be due to multiple factors, including mechanical and structural properties of TVPs (Deng, Mars, Van Der Sman, Smeets, & Janssen, 2020; Liu et al., 2024; Luo, Borst, Westphal, Boom, & Janssen, 2017; Luo, Zhan, Boom, & Janssen, 2018). Our previous study measured the mechanical properties of TVP-based patties (Young's modulus, yield stress and strain) (van Esbroeck et al., 2024) (Supplementary Table 3). These results might roughly indicate

**Table 2**
Surface area, water absorption capacity (WAC) after 30 min incubation of dry TVP, WAC at pH 2 after 30 min incubation of rehydrated TVP and acid absorption properties of rehydrated TVP powders, rehydrated TVPs and TVP patties at 5 min and 120 min. Data (mean ± SD, n = 5 for the surface area of TVP and patty, n = 2 for other measurements) with different superscript letters in a column are significantly different ($p < 0.05$). †The surface areas of dry TVP powders include the microscopic surface area caused by potential nanopores presented in power particles, whereas the surface areas of rehydrated TVPs and patties only represent the macroscopic surface area determined based on 2D images. *data reported by van Esbroeck et al. (2024).

| | Surface area† | | | WAC (%)* | WAC (%) at pH2 | Acid absorption (mmol) at 5 min without pepsin | | | Acid absorption (mmol) at 120 min without pepsin | | |
|---|---|---|---|---|---|---|---|---|---|---|---|
| | powder ($m^2/g$) | TVP ($mm^2/g$) | patty ($mm^2/g$) | dry TVP | TVP | powder | TVP | patty | powder | TVP | patty |
| ROQ1 | $231\pm3^{d}$ | $809 \pm 27^{b}$ | $656 \pm 25^{a}$ | $397 \pm 6^{c}$ | $113 \pm 11^{a}$ | $1.10 \pm 0.08^{abc}$ | $0.63 \pm 0.04^{ab}$ | $0.41 \pm 0.16^{ab}$ | $1.18 \pm 0.1$ | $1.41 \pm 0.55$ | $0.99 \pm 0.12^{ab}$ |
| ROQ2 | $183\pm0^{ab}$ | $1140 \pm 97^{de}$ | $837 \pm 99^{b}$ | $336 \pm 4^{b}$ | $161 \pm 27^{ab}$ | $1.10 \pm 0.07^{abc}$ | $0.78 \pm 0.16^{ab}$ | $0.40 \pm 0.21^{ab}$ | $1.18 \pm 0.02$ | $1.14 \pm 0.1$ | $0.98 \pm 0.15^{ab}$ |
| ROQ3 | $223\pm2^{cd}$ | $1164 \pm 51^{e}$ | $1055 \pm 54^{d}$ | $709 \pm 7^{e}$ | $336 \pm 96^{b}$ | $1.12 \pm 0.08^{abcd}$ | $0.90 \pm 0.05^{bc}$ | $0.60 \pm 0.09^{ab}$ | $1.31 \pm 0.2$ | $1.20 \pm 0.08$ | $1.03\pm0^{ab}$ |
| ROQ5 | $202\pm2^{bc}$ | $1040 \pm 31^{cd}$ | $900 \pm 38^{bc}$ | $488 \pm 16^{d}$ | $128 \pm 17^{a}$ | $0.95 \pm 0.08^{a}$ | $0.75 \pm 0.07^{ab}$ | $0.35 \pm 0.07^{ab}$ | $1.10 \pm 0.14$ | $1.14 \pm 0.02$ | $0.89 \pm 0.07^{a}$ |
| VEG1 | $167\pm1^{a}$ | $988 \pm 42^{c}$ | $811 \pm 49^{b}$ | $401 \pm 2^{c}$ | $116\pm7^{a}$ | $1.33 \pm 0.04^{cde}$ | $0.89 \pm 0.05^{abc}$ | $0.56 \pm 0.03^{ab}$ | $1.38 \pm 0.03$ | $1.29 \pm 0.06$ | $1.12 \pm 0.02^{ab}$ |
| VEG2 | $181 \pm 11^{a}$ | $1294 \pm 43^{f}$ | $1011 \pm 59^{cd}$ | $134 \pm 6^{a}$ | $191 \pm 63^{ab}$ | $1.34 \pm 0.02^{de}$ | $1.12 \pm 0.04^{c}$ | $0.83 \pm 0.12^{bc}$ | $1.40 \pm 0.03$ | $1.52 \pm 0.05$ | $1.29 \pm 0.12^{b}$ |
| GMI1 | $179\pm0^{a}$ | $558 \pm 16^{a}$ | $561 \pm 36^{a}$ | $298 \pm 28^{b}$ | $120 \pm 12^{a}$ | $1.36 \pm 0.04^{e}$ | $0.60 \pm 0.08^{a}$ | $0.56 \pm 0.02^{ab}$ | $1.37 \pm 0.03$ | $1.27 \pm 0.07$ | $1.14 \pm 0.03^{ab}$ |
| GMI2 | $164 \pm 10^{a}$ | $1740 \pm 97^{g}$ | $1226 \pm 54^{e}$ | $533 \pm 3^{d}$ | $247 \pm 42^{ab}$ | $1.28 \pm 0.04^{bcde}$ | $1.18 \pm 0.03^{c}$ | $1.22 \pm 0.01^{c}$ | $1.29 \pm 0.06$ | $1.31 \pm 0.03$ | $1.28 \pm 0.01^{b}$ |

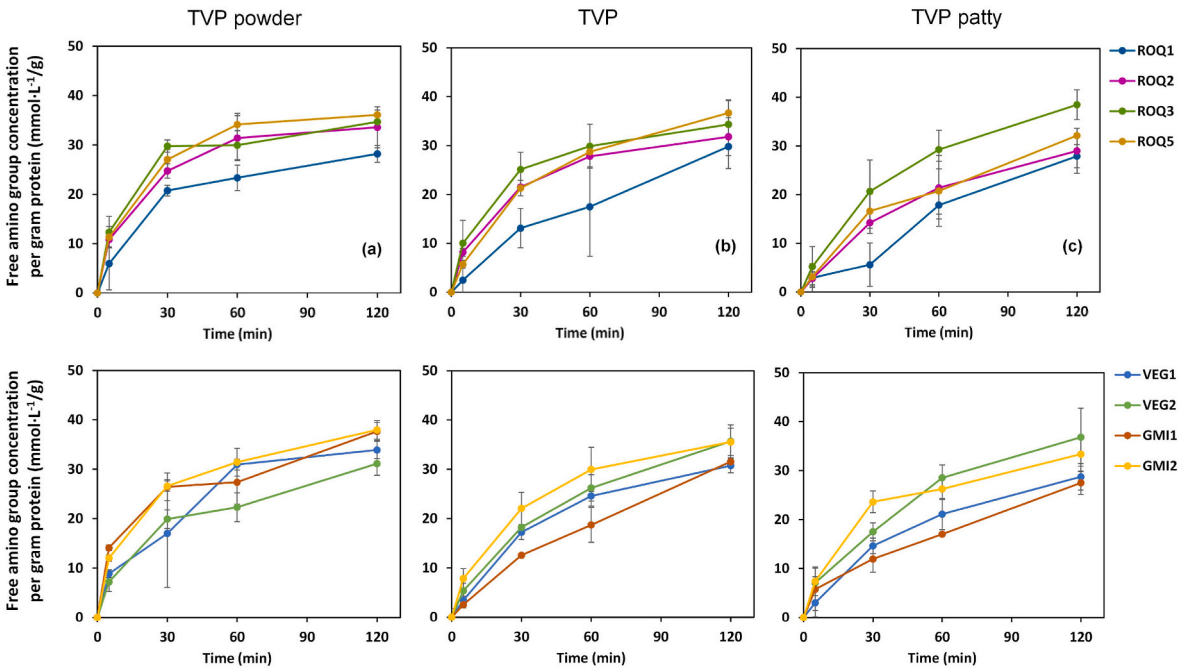


**Fig. 1.** Free amino group concentration per gram protein in gastric juice during *in vitro* gastric protein digestion of rehydrated TVP powders, TVPs (rehydrated and intact), and TVP patties. First row: yellow pea; second row: soybean. Error bars denote standard deviations (n = 2).

the mechanical properties of TVPs and TVP-based patties in this study. For example, patties prepared from GMI2 (Young's modulus = 7 kPa) were likely softer than patties prepared from VEG1 (Young's modulus = 37 kPa). This might partially explain the higher free amino group concentration observed during the digestion of TVP patties for GMI2 compared to VEG1 (Liu et al., 2024). However, the impact of mechanical properties on protein digestion can interact with microstructure (Liu et al., 2024). During the digestion of TVP patties, ROQ3 showed higher free amino group concentrations than ROQ2, despite their similar mechanical properties (Supplementary Table 3). Therefore, other factors, such as surface area, structural properties, water and acid absorption capacity contributed to the differences in free amino group concentrations. The impact of these factors on protein hydrolysis during *in vitro* gastric digestion of rehydrated TVP powders, rehydrated intact TVPs and patties is further analyzed and discussed in the following section. It is noted that the oral phase of digestion was omitted in this study. The macrostructural breakdown during mastication and mixing with simulated saliva fluid could have changed the structural properties of TVPs and consequently could have impacted the *in vitro* gastric digestion. Future studies are needed to explore the combined effect of initial TVP structure, TVP micro- and macrostructure after mastication and oral structural breakdown on the *in vitro* gastric digestion of TVPs and TVP-based meat analogues.

### *3.3. Impact of structural properties, water absorption and acid absorption on in vitro gastric protein digestion of TVP powders, intact TVPs and patties*

#### *3.3.1. Surface area*

For TVP powders, no significant correlations between surface area and protein hydrolysis were observed (Fig. 2a). This was attributed to the relatively limited variability in surface area (164–231 $m^2/g$)

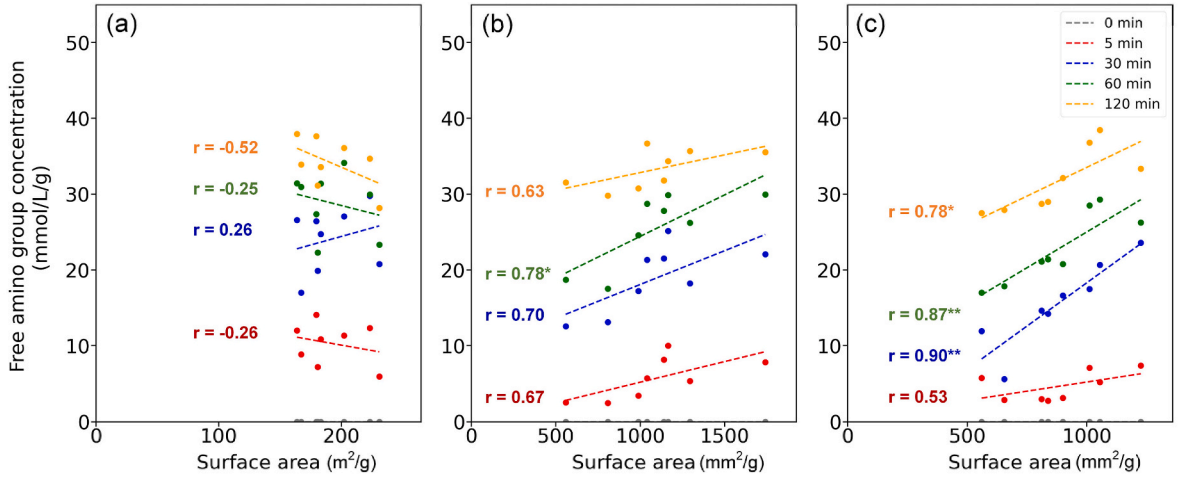


**Fig. 2.** Scatter plots of free amino group concentrations during *in vitro* gastric protein digestion of (a) rehydrated TVP powders, (b) rehydrated intact TVPs and (c) TVP-based patties against the surface area of TVP powders, rehydrated TVPs and separated particles of TVP-based patties. r refers to the Pearson correlation coefficient. *Correlation is significant at the 0.05 level; **. Correlation is significant at the 0.01 level.

between TVP powders. Significant positive correlations between surface area and free amino group concentrations were found during the digestion of rehydrated intact TVPs at 60 min ($p = 0.022$) (Fig. 2b). This result is consistent with previous studies which reported that an increase in surface area of protein gels strongly promoted *in vitro* gastric protein digestion (Guo et al., 2015; Liu et al., 2024; Markussen, Madsen, Young, & Corredig, 2021). Interestingly, these significant correlations were also found during the digestion of patties at 30 min ($p = 0.002$), 60 min ($p = 0.005$) and 120 min ($p = 0.022$) (Fig. 2c). This result indicates that the addition of other ingredients and the cooking process during patty preparation did not change the fact that increasing surface area of food particles facilitated protein hydrolysis. It should be mentioned that, for rehydrated intact TVPs and patties, the microscopic surface area provided by pores in the microstructure of TVPs is not considered here, but is discussed in section 3.3.2.

### 3.3.2. Mean pore size and XRT-based porosity

There were no significant correlations between mean pore size and free amino group concentrations during the digestion of TVP powders (Fig. 3a). This was expected, as the porous structure of TVPs was removed by milling. For intact TVP, mean pore size was significantly and positively correlated with free amino group concentrations during the digestion, with the highest correlation at 5 min ($p = 0.038$). Such a correlation was also seen for patties for 5 ($p = 0.038$), 30 ($p = 0.019$) and 60 min ($p = 0.016$) (Fig. 3), where 60 min had the highest correlation.

This finding suggests that large pores in TVPs facilitated protein hydrolysis during the *in vitro* gastric digestion of rehydrated intact TVPs, and this impact of pore size on protein digestion persisted in TVP patties. This result is consistent with the result of Azzollini et al. (2018), who reported positive correlations between pore size and the *in vitro* protein and starch digestibility of extruded insect-enriched wheat snacks. It is noted that for TVPs with large mean pore size, they also exhibited large surface area after rehydration (Table 2). The significant positive correlations between mean pore size and free amino group concentrations during the digestion of rehydrated TVPs and patties might partly be caused by the correlation between mean pore size and the surface area of rehydrated TVPs. Nevertheless, the impact of mean pore size on protein hydrolysis should not be disregarded. The correlations between structural properties and water or acid absorption shown in Supplementary Table 4 provide evidence for this point. Significant positive correlations were found between mean pore size and water absorption capacity of rehydrated TVPs at pH 2 ($r = 0.82$, $p = 0.013$), between mean pore size and acid absorption at 5 min of rehydrated TVPs ($r = 0.81$, $p = 0.014$) and patties ($r = 0.87$, $p = 0.011$), whereas no significant correlations were found between surface area and water absorption or acid absorption except the acid absorption at 5 min of rehydrated TVPs ($r = 0.91$, $p = 0.002$). These results imply that despite its correlation with surface area, large mean pore size could promote the protein hydrolysis of rehydrated TVPs and patties by increasing the water absorption capacity of TVPs at pH 2 and the acid absorption of TVPs and patties. In addition, large pore size could accelerate the diffusion of pepsin in TVP particles. Faster pepsin diffusion was observed in dairy gels, egg white gels and myofibrillar protein gels with larger pore size, resulting in higher degree of protein hydrolysis (Luo et al., 2017; Somaratne et al., 2020; Thévenot, Cauty, Legland, Dupont, & Floury, 2017; Zhang et al., 2023). For intact TVPs, the positive correlation between mean pore size and protein hydrolysis was significant only at 5 min (Fig. 3b). This might be attributed to the structure disintegration caused by digestion. The delayed and prolonged impact of pore size on protein hydrolysis during the digestion of patties (Fig. 3c) might be due to the addition of other ingredients such as sunflower oil, pea protein isolate, and methylcellulose. At the beginning of the digestion (the first 5 min), these ingredients might spatially hinder the penetration and diffusion of pepsin into TVPs, as well as acid absorption (Zuo et al., 2024). This study focused on the correlations between initial structures of TVPs and *in vitro* gastric digestion of TVPs-based patties. Further studies are needed to explore the impact of structural changes in TVPs caused by digestion and/or the addition of other ingredients on digestion kinetics.

Porosity of TVPs measured by XRT did not significantly correlate with free amino group concentrations during the *in vitro* gastric digestion of rehydrated TVP powders, rehydrated intact TVPs and patties (Fig. 4). The determination of XRT-based porosity was volume-based, while the determination of mean pore size was based on the detected distances between each air pixel and the nearest wall (van Esbroeck et al., 2024). Therefore, XRT-based porosity could be influenced by the volume of walls present in TVPs, while mean pore size depends purely on pore size. For example, ROQ1 and ROQ3 had similar XRT-based porosity (64% and 66%), but ROQ1 had a significantly smaller mean pore size (526 μm) than ROQ3 (1921 μm), which is in accordance with the XRT images showing more large pores in ROQ3 than in ROQ1 (Supplementary Fig. 1). The porosity of TVPs measured by XRT thus contributed less to protein hydrolysis during *in vitro* gastric digestion of rehydrated TVPs and patties. TVP pore size promoted protein digestion more than TVP porosity.

### 3.3.3. Mean wall thickness and wall density

Mean wall thickness was not significantly correlated with the free amino group concentrations (Supplementary Table 5), which was attributed to the extremely large mean wall thickness of VEG2 and

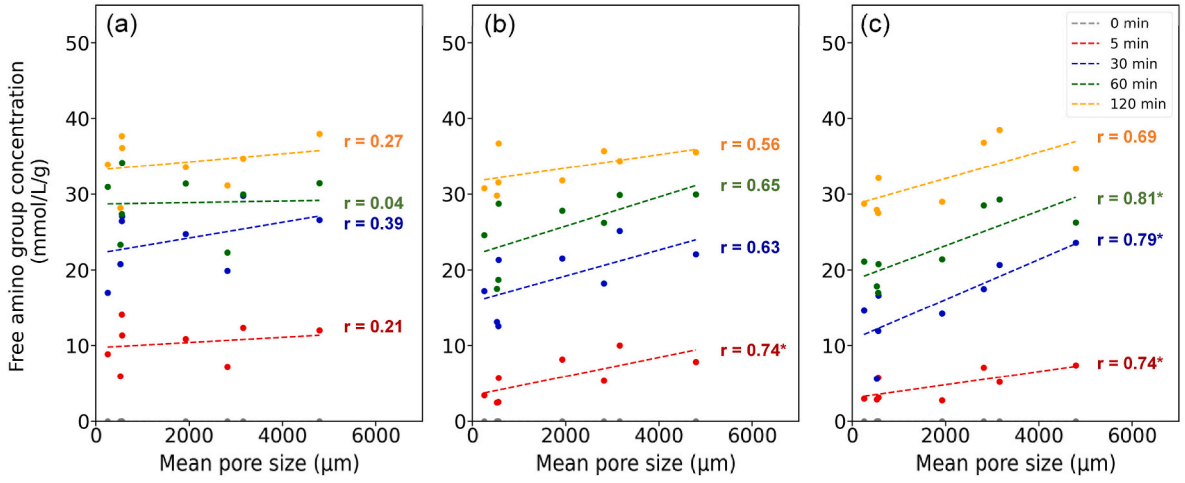


**Fig. 3.** Scatter plots of free amino group concentrations during *in vitro* gastric protein digestion of (a) rehydrated TVP powders, (b) rehydrated TVPs and (c) TVP-based patties against the mean pore size measured by XRT of dry TVPs. r refers to the Pearson correlation coefficient. *Correlation is significant at the 0.05 level.

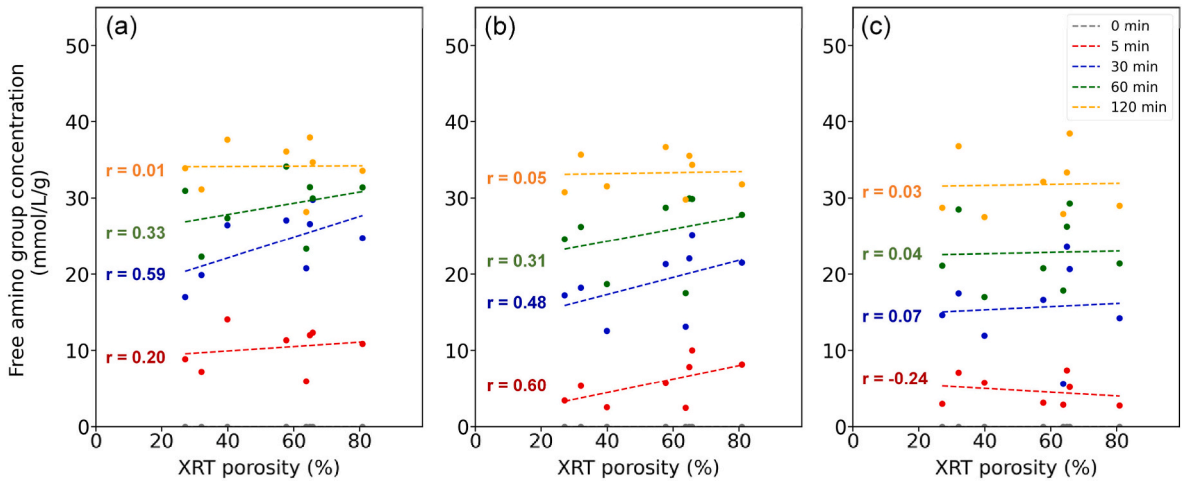


**Fig. 4.** Scatter plots of free amino group concentrations during *in vitro* gastric protein digestion of (a) rehydrated TVP powders, (b) rehydrated TVPs and (c) TVP-based patties against the porosity measured by XRT of dry TVPs. r refers to the Pearson correlation coefficient.

relatively small variability in mean wall thickness of all other samples (Table 1). Wall density was negatively correlated with the free amino group concentrations during the *in vitro* gastric digestion of TVP powders at 5 min ($p = 0.021$) and 30 min ($p = 0.002$) (Fig. 5a). This could explain the differences in free amino group concentrations among TVP powders (Fig. 1). Even though TVPs were ground into fine powders, differences in wall density of TVPs might still be present. Higher wall density suggests a more compact and dense protein network, which hinders the diffusion of pepsins in the protein network of TVPs, resulting in less protein hydrolysis. The resistance of a dense protein network to protein hydrolysis was also found in whey protein and myofibrillar protein gels (Liu et al., 2024; Singh, Øiseth, Lundin, & Day, 2014; Zhang et al., 2023). Gels with a heterogeneous microstructure were digested slower than those with a homogeneous microstructure, which was attributed to the dense protein aggregates in the protein-rich phase. However, the negative correlations between wall density and free amino group concentrations were not significant ($p > 0.05$) for intact TVPs and patties (Fig. 5). This may suggest that, when porous structures are present in the TVPs, pore size, rather than wall density, is the primary structural property determining protein hydrolysis during the digestion of TVPs and TVP-based patties. This could be because pore size contributes to the protein hydrolysis at the microscopic surface of TVPs, whereas wall density affects the diffusion of pepsins inside the walls. Once pepsin reaches the pores, protein hydrolysis starts from the surface of solid materials (walls, in case of TVPs), which was also reported for whey protein gels during *in vitro* gastric protein digestion (Deng et al., 2020; Luo et al., 2017). Furthermore, the disintegration of whey protein gels was shown to be dominated by surface erosion (Guo et al., 2015). The *in vitro* gastric protein digestion of TVPs seemingly followed a similar disintegration mechanism as for the whey protein gels. As discussed before, large pores in TVPs could accelerate the dispersing of pepsin between walls and enhance the absorption of water and acid, boosting the protein hydrolysis and the erosion at the microscopic surface of TVPs (the surface of walls in TVPs). Therefore, wall density, which influences the diffusion of pepsins inside walls rather than the protein hydrolysis at the wall surface, contributed less to the protein digestion of intact TVPs and TVP-based patties than pore size.

### 3.3.4. *Apparent density, absolute density and density-based porosity*

Apparent density, absolute density and density-based porosity were not correlated with the free amino group concentrations during *in vitro* gastric protein digestion of TVPs and patties (Supplementary Table 5). However, when VEG1 and VEG2, which had very low density-based porosity and very high apparent density (Table 1), were excluded from the data set, significant negative correlations were found between apparent density and the protein hydrolysis of TVPs and patties (Fig. 6, the top row). Correspondingly, positive correlations were found between density-based porosity and the protein hydrolysis of TVPs and patties (Fig. 6, the bottom row). The fact that VEG1 and VEG2 were outliers could be attributed to variations in extrusion cooking, which may also have caused the obvious darker color of the TVPs (Supplementary Table 1). These high correlations without VEG samples indicate that density-based porosity and apparent density were positively and negatively correlated with protein hydrolysis during the *in*

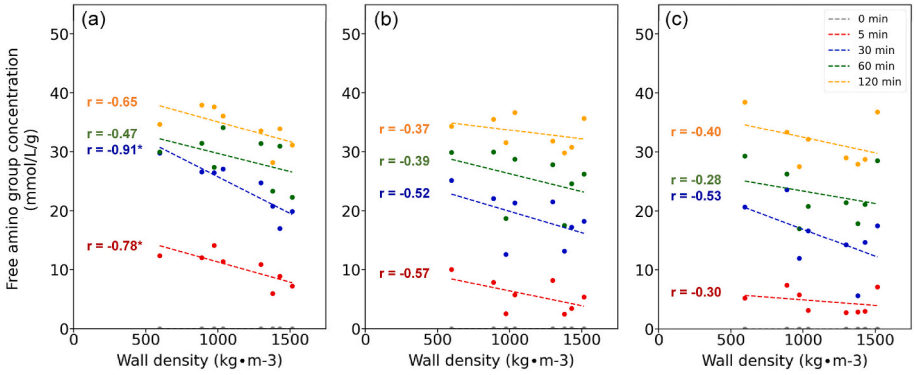


**Fig. 5.** Scatter plots of free amino group concentrations during *in vitro* gastric protein digestion of (a) rehydrated TVP powders, (b) rehydrated TVPs and (c) TVP-based patties against the wall density of dry TVPs. r refers to the Pearson correlation coefficient. *Correlation is significant at the 0.05 level.

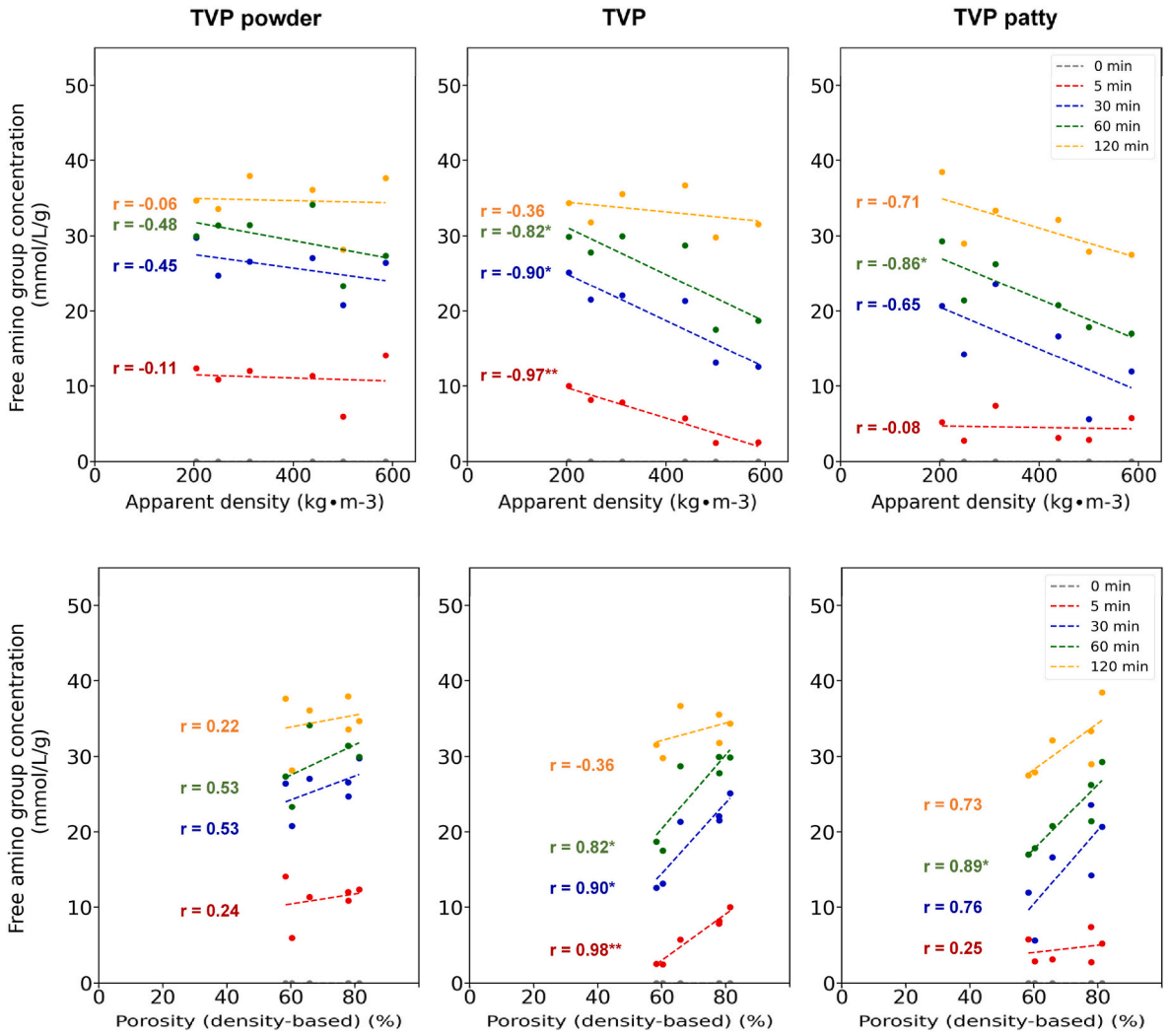


**Fig. 6.** Scatter plots of free amino group concentrations during *in vitro* gastric protein digestion of rehydrated TVP powders, TVPs (rehydrated and intact), and TVP patties against the apparent density and density-based porosity of dry TVPs. Note: VEG1 and VEG2 are excluded. r refers to the Pearson correlation coefficient. *Correlation is significant at the 0.05 level. **Correlation is significant at the 0.01 level.

*vitro* gastric digestion of TVPs and TVP-based patties, respectively. These results are inconsistent with that of Lin et al. (2022, 2023) who reported larger extent of protein digestion during *in vitro* gastrointestinal digestion of textured wheat proteins (TWPs) with larger bulk density. The TWPs tested by Lin et al. displayed fibrous microstructure instead of a porous structure as shown in this study, which might be due to the variation in the moisture content during extrusion. The larger degree of protein digestion of TWPs was attributed to the finer fibers and greater exposure of hydrophobic groups in protein molecules with no explanation about the influence of bulk density (Lin et al., 2022, 2023). In this study, the apparent density of TVPs was positively correlated with the wall thickness ($r = 0.756$, $p = 0.030$) and the wall density ($r = 0.708$, $p = 0.050$), and negatively correlated with the porosity measured by XRT ($r = -0.920$, $p = 0.001$) and, of course, the density-based porosity ($r = -0.997$, $p < 0.001$). Therefore, the impact of apparent density and density-based porosity can be seen as the combined effect of pores and walls of TVPs on protein hydrolysis during the digestion of intact TVPs and TVP-based patties. Regarding the exceptions of VEG1 and VEG2, further studies are needed to explore the impact of compact structures of TVPs on their gastric protein digestion, with consideration of extrusion conditions.

### 3.3.5. *Water absorption and acid absorption*

As protein hydrolysis is expected to be related to the ease of water and acid uptake by samples during digestion, we evaluated the correlation between water absorption capacity and free amino group concentrations, as well as between acid absorption (with and without pepsin) and free amino group concentrations (Supplementary Table 5).

The WAC of rehydrated TVPs at pH 2 was positively correlated with the free amino group concentrations during *in vitro* gastric digestion of intact TVPs and patties (Fig. 7). These results confirm that increasing in WAC of rehydrated TVPs at pH 2 facilitated the protein hydrolysis during *in vitro* gastric digestion of TVPs and TVP-based patties. This is consistent with the results of Deng et al. (2020), who studied the impact of swelling on the *in vitro* gastric protein digestion of whey protein gels. They concluded that swelling, i.e. water absorption, increased the digestion rate of whey protein gels by enhancing acid diffusion and pepsin partitioning at the gel-liquid interface. In our study, we can observe that the impact of WAC at pH 2 in TVPs appeared larger during the first 30 min, whereas in patties, the impact became larger in the period between 30 and 120 min (higher correlations). This was likely due to the presence of additional ingredients in the patties, such as fat, which might occupy the pores in TVPs, reducing the accessibility of gastric juice to the porous structure in early stages of digestion (Zuo et al., 2024). No correlation was found between WAC of dry TVPs at

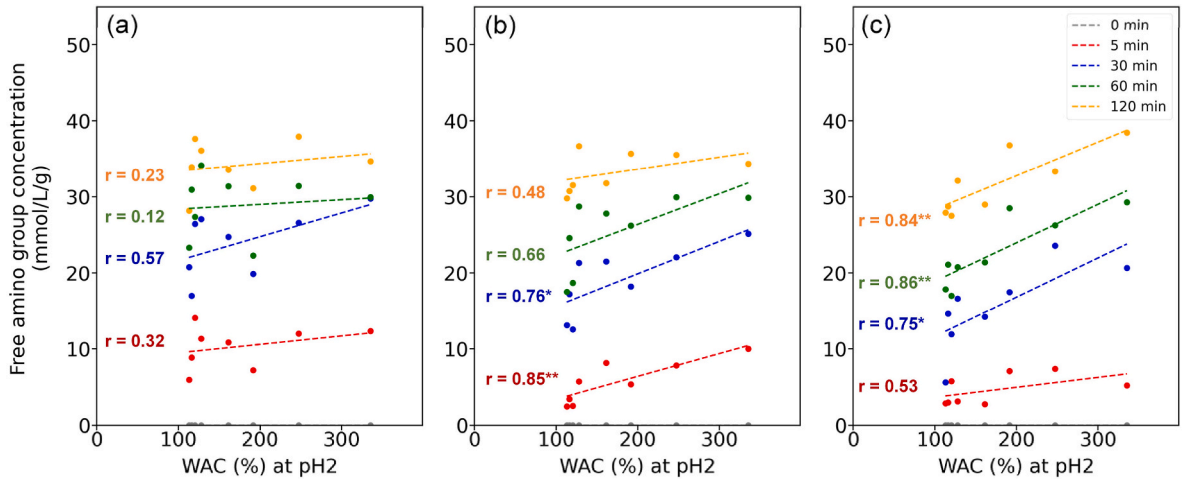


**Fig. 7.** Scatter plots of free amino group concentrations during *in vitro* gastric protein digestion of (a) rehydrated TVP powders, (b) rehydrated TVPs and (c) TVP-based patties against the water absorption capacity at pH 2 of rehydrated TVP powders, rehydrated TVPs and separated particles of TVP-based patties. r refers to the Pearson correlation coefficient. *Correlation is significant at the 0.05 level; ** Correlation is significant at the 0.01 level.

neutral pH and the free amino group concentrations during digestion of TVP powders, TVPs and patties (Supplementary Table 5). This result suggests that the typical WAC of dry TVPs in water at neutral pH is less relevant to the digestibility of TVPs during gastric digestion. When the WAC of TVPs is manipulated in order to improve the digestibility of TVPs, WAC should be determined under digestion conditions (in simulated gastric juice at pH 2 without pepsin) rather than in water at neutral pH.

Regarding acid absorption, positive correlations between acid absorption in the absence of pepsin and free amino group concentrations were found for patties at 5 min of digestion (Supplementary Table 5). This indicates that the increased acid absorption capacity of TVP patties facilitated the protein hydrolysis of patties at the beginning of digestion. There were no significant correlations between acid absorption in the absence of pepsin and protein hydrolysis for intact TVPs (Supplementary Table 5). The acid consumption during digestion with pepsin also did not significantly correlate with the free amino group concentrations during the digestion of intact TVPs. These results imply that despite the significant positive correlations between mean pore size and acid absorption (Supplementary Table 4), the increased acid absorption was not the dominant reason for promoted protein hydrolysis of TVPs with large pores. This finding supports our assumption in section 3.3.2 and section 3.3.3 that, apart from water and acid absorption, pepsin diffusion within TVP particles could also be affected by TVP structural properties, thereby influencing the protein hydrolysis during TVP digestion. Further studies exploring the impact of structural properties of TVPs on pepsin penetrating and diffusion during the protein digestion of TVP-based meat analogues could gain more insight into this aspect.

## 4. Conclusions

This study evaluated the impact of structural properties of texture vegetable proteins (TVPs) on the *in vitro* gastric protein digestion of TVPs and TVP-based patties in a quantitative way. The macrostructure of TVPS, represented by the surface area, and microscopic structural properties such as mean pore size, wall density, apparent density, density-based porosity, are relevant for protein hydrolysis during *in vitro* gastric digestion of rehydrated TVPs. Other structural properties including porosity measured by XRT, mean wall thickness and absolute density are less relevant. Increased macroscopic surface area, mean pore size and density-based porosity gave rise to faster protein hydrolysis during digestion of TVPs, whereas increased apparent density of TVPs slowed down protein hydrolysis. These correlations persisted for patties prepared from these TVPs, although correlations were often more pronounced at later stages during digestion. It is worth noting that the negative correlation between wall density and protein hydrolysis was observed only when the porous structure of TVPs was removed. The lack of such correlations for intact TVP and patties suggests that the impact of microscopic structural properties on protein digestion of TVPs and patties was more dominated by pore-related TVP properties rather than wall-related TVP properties. Pores in TVPs influenced water absorption capacity at pH 2 and acid absorption, which influenced the protein digestion of TVPs and TVP-based patties. We suggest that for enhancing protein digestion of TVP-based meat analogues, increasing the pore size of TVPs with a porous structure and decreasing the wall density of TVPs with a compact structure should be considered in addition to increasing macroscopic surface area (i.e. reducing the particle size) of TVPs. Future studies should explore the relationships between structural properties and protein digestion of meat analogues made from TVPs with compact, fibrous microstructure taking extrusion conditions and pepsin diffusion into consideration.

## CRediT authorship contribution statement

**Dan Liu:** Writing – review & editing, Writing – original draft, Visualization, Project administration, Methodology, Investigation, Formal analysis, Data curation, Conceptualization. **Thiemo van Esbroeck:** Writing – review & editing, Visualization, Methodology, Investigation, Data curation, Conceptualization. **Anja E.M. Janssen:** Writing – review & editing, Supervision, Resources, Project administration, Methodology, Conceptualization. **Elke Scholten:** Writing – review & editing, Supervision, Resources, Project administration, Methodology, Conceptualization. **Paul A.M. Smeets:** Writing – review & editing, Supervision, Resources, Project administration, Methodology, Conceptualization. **Markus Stieger:** Writing – review & editing, Supervision, Resources, Project administration, Methodology, Funding acquisition, Conceptualization.

## Declaration of competing interest

The authors declare that they have no known competing financial interests or personal relationships that could have appeared to influence the work reported in this paper.

## Acknowledgements

D.L. acknowledges financial support by the China Scholarship Council (Grant No. 202006300007). The authors thank Gabriella

Averina Utomo Putri and Nienke Keijzer for helping with data collection.

## Appendix A. Supplementary data

Supplementary data to this article can be found online at https://doi.org/10.1016/j.foodhyd.2024.111011.

## Data availability

Data will be made available on request.

## References


Azzollini, D., Derossi, A., Fogliano, V., Lakemond, C. M. M., & Severini, C. (2018). Effects of formulation and process conditions on microstructure, texture and digestibility of extruded insect-riched snacks. *Innovative Food Science and Emerging Technologies, 45*, 344–353. https://doi.org/10.1016/j.ifset.2017.11.017

Barbé, F., Ménard, O., Le Gouar, Y., Buffière, C., Famelart, M. H., Laroche, B., et al. (2013). The heat treatment and the gelation are strong determinants of the kinetics of milk proteins digestion and of the peripheral availability of amino acids. *Food Chemistry, 136*(3–4), 1203–1212. https://doi.org/10.1016/J.FOODCHEM.2012.09.022

Baune, M. C., Terjung, N., Tülbek, M.Ç., & Boukid, F. (2022). Textured vegetable proteins (TVP): Future foods standing on their merits as meat alternatives. *Future Foods, 6*. https://doi.org/10.1016/j.fufo.2022.100181

Brishti, F. H., Chay, S. Y., Muhammad, K., Ismail-Fitry, M. R., Zarei, M., & Saari, N. (2021). Texturized mung bean protein as a sustainable food source: Effects of extrusion on its physical, textural and protein quality. *Innovative Food Science and Emerging Technologies, 67*. https://doi.org/10.1016/j.ifset.2020.102591

Brodkorb, A., Egger, L., Alminger, M., Alvito, P., Assunção, R., Ballance, S., et al. (2019). INFOGEST static in vitro simulation of gastrointestinal food digestion. *Nature Protocols, 14*(4), 991–1014. https://doi.org/10.1038/s41596-018-0119-1

Capuano, E., & Janssen, A. E. M. (2021). Food matrix and macronutrient digestion. *Annual Review of Food Science and Technology, 12*, 193–212. https://doi.org/10.1146/annurev-food-032519-051646

Chen, Y., Capuano, E., & Stieger, M. (2021). Chew on it: Influence of oral processing behaviour on in vitro protein digestion of chicken and soya-based vegetarian chicken. *British Journal of Nutrition, 126*(9), 1408–1419. https://doi.org/10.1017/S0007114520005176

Del Rio, A. R., Boom, R. M., & Janssen, A. E. M. (2022). Effect of fractionation and processing conditions on the digestibility of plant proteins as food ingredients. *Foods, 11*(6). https://doi.org/10.3390/foods11060870. MDPI.

Deng, R., Mars, M., Van Der Sman, R. G. M., Smeets, P. A. M., & Janssen, A. E. M. (2020). The importance of swelling for in vitro gastric digestion of whey protein gels. *Food Chemistry, 330*, Article 127182. https://doi.org/10.1016/j.foodchem.2020.127182

Flory, J., & Alavi, S. (2024). Use of hydration properties of proteins to understand their functionality and tailor texture of extruded plant-based meat analogues. *Journal of Food Science, 89*(1), 245–258. https://doi.org/10.1111/1750-3841.16804

Gorissen, S. H. M., Crombag, J. J. R., Senden, J. M. G., Waterval, W. A. H., Bierau, J., Verdijk, L. B., et al. (2018). Protein content and amino acid composition of commercially available plant-based protein isolates. *Amino Acids, 50*(12), 1685–1695. https://doi.org/10.1007/s00726-018-2640-5

Guo, Q., Ye, A., Lad, M., Ferrua, M., Dalgleish, D., & Singh, H. (2015). *Disintegration kinetics of food gels during gastric digestion and its role on gastric emptying: An in vitro analysis* (Vol. 6, p. 756). https://doi.org/10.1039/c4fo00700j

Hong, S., Shen, Y., & Li, Y. (2022). Physicochemical and functional properties of texturized vegetable proteins and cooked patty textures: Comprehensive characterization and correlation analysis. *Foods, 11*(17). https://doi.org/10.3390/foods11172619

Imran, M., & Liyan, Z. (2023). Production of plant-based meat: Functionality, limitations and future prospects. *European Food Research and Technology, 249*(9), 2189–2213. https://doi.org/10.1007/s00217-023-04287-w

Ishaq, A., Irfan, S., Sameen, A., & Khalid, N. (2022). Plant-based meat analogs: A review with reference to formulation and gastrointestinal fate. *Current Research in Food Science, 5*, 973–983. https://doi.org/10.1016/j.crfs.2022.06.001. Elsevier B.V.

Jeon, Y. H., Gu, B. J., & Ryu, G. H. (2023). Investigating the potential of full-fat soy as an alternative ingredient in the manufacture of low- and high-moisture meat analogs. *Foods, 12*(5). https://doi.org/10.3390/foods12051011

Kaur, L., Mao, B., Beniwal, A. S., Abhilasha, Kaur, R., Chian, F. M., et al. (2022). Alternative proteins vs animal proteins: The influence of structure and processing on their gastro-small intestinal digestion. *Trends in Food Science and Technology, 122*, 275–286. https://doi.org/10.1016/j.tifs.2022.02.021

Kong, F., & Singh, R. P. (2008). Disintegration of solid foods in human stomach. *Journal of Food Science, 73*(5), R67–R80. https://doi.org/10.1111/j.1750-3841.2008.00766.x

Lin, Q., Pan, L., Deng, N., Sang, M., Cai, K., Chen, C., et al. (2022). Protein digestibility of textured-wheat-protein (TWP) -based meat analogues: (I) effects of fibrous structure. *Food Hydrocolloids, 130*. https://doi.org/10.1016/j.foodhyd.2022.107694

Lin, Q., Sang, M., Jin, H., Huang, D., Zhang, Y., Han, J., et al. (2023). Protein digestibility of textured wheat protein (TWP)-based meat analogs: (II) effects of sodium tripolyphosphate. *Food Research International, 173*. https://doi.org/10.1016/j.foodres.2023.113280

Liu, D., Janssen, A. E. M., Smeets, P. A. M., & Stieger, M. (2024a). Interplay between microstructure, mechanical properties, macrostructure breakdown and in vitro gastric digestion of whey protein gels. *Food Hydrocolloids, 147*, Article 109352. https://doi.org/10.1016/j.foodhyd.2023.109352

Liu, D., Janssen, A. E. M., Smeets, P. A. M., & Stieger, M. (2024b). Impact of microstructure of whey protein gels on in vitro gastric protein digestion is sustained after oral structural breakdown by mastication. *Food Hydrocolloids, 159*, Article 110619. https://doi.org/10.1016/j.foodhyd.2024.110619

Luo, Q., Borst, J. W., Westphal, A. H., Boom, R. M., & Janssen, A. E. M. (2017). Pepsin diffusivity in whey protein gels and its effect on gastric digestion. *Food Hydrocolloids, 66*, 318–325. https://doi.org/10.1016/j.foodhyd.2016.11.046

Luo, Q., Zhan, W., Boom, R. M., & Janssen, A. E. M. (2018). Interactions between acid and proteins under in vitro gastric condition-a theoretical and experimental quantification. *Food & Function, 9*(10), 5283–5289. https://doi.org/10.1039/C8FO01033A

Markussen, J.Ø., Madsen, F., Young, J. F., & Corredig, M. (2021). A semi dynamic in vitro digestion study of milk protein concentrate dispersions structured with different polysaccharides. *Current Research in Food Science, 4*, 250–261. https://doi.org/10.1016/j.crfs.2021.03.012

Mennah-Govela, Y. A., & Bornhorst, G. M. (2021). Breakdown mechanisms of whey protein gels during dynamic in vitro gastric digestion. *Food & Function, 12*(5), 2112–2125. https://doi.org/10.1039/d0fo03325a

Nielsen, P. M., Petersen, D., & Dambmann, C. (2001). Improved method for determining food protein degree of hydrolysis. *Journal of Food Science, 66*(5), 642–646. https://doi.org/10.1111/j.1365-2621.2001.tb04614.x

Sá, A. G. A., Moreno, Y. M. F., & Carciofi, B. A. M. (2020). Food processing for the improvement of plant proteins digestibility. *Critical Reviews in Food Science and Nutrition, 60*(20), 3367–3386. https://doi.org/10.1080/10408398.2019.1688249

Samard, S., Gu, B. Y., & Ryu, G. H. (2019). Effects of extrusion types, screw speed and addition of wheat gluten on physicochemical characteristics and cooking stability of meat analogues. *Journal of the Science of Food and Agriculture, 99*(11), 4922–4931. https://doi.org/10.1002/jsfa.9722

Samard, S., Maung, T. T., Gu, B. Y., Kim, M. H., & Ryu, G. H. (2021). Influences of extrusion parameters on physicochemical properties of textured vegetable proteins and its meatless burger patty. *Food Science and Biotechnology, 30*(3), 395–403. https://doi.org/10.1007/s10068-021-00879-y

Singh, T. K., Øiseth, S. K., Lundin, L., & Day, L. (2014). Influence of heat and shear induced protein aggregation on the in vitro digestion rate of whey proteins. *Food & Function, 5*. https://doi.org/10.1039/c4fo00454j

Somaratne, G., Nau, F., Ferrua, M. J., Singh, J., Ye, A., Dupont, D., et al. (2020). Characterization of egg white gel microstructure and its relationship with pepsin diffusivity. *Food Hydrocolloids, 98*, Article 105258. https://doi.org/10.1016/j.foodhyd.2019.105258

Thévenot, J., Cauty, C., Legland, D., Dupont, D., & Floury, J. (2017). Pepsin diffusion in dairy gels depends on casein concentration and microstructure. *Food Chemistry, 223*, 54–61. https://doi.org/10.1016/j.foodchem.2016.12.014

van Esbroeck, T., Sala, G., Stieger, M., & Scholten, E. (2024). Effect of structural characteristics on functional properties of textured vegetable proteins. *Food Hydrocolloids, 149*. https://doi.org/10.1016/j.foodhyd.2023.109529

Wang, Y., Zheng, Z., Zhang, C., Wu, C., Tan, C. P., & Liu, Y. (2024). Comparative structural, digestion and absorption characterization of three common extruded plant proteins. *Food Research International, 177*. https://doi.org/10.1016/j.foodres.2023.113852

Xie, Y., Cai, L., Zhao, D., Liu, H., Xu, X., Zhou, G., et al. (2022). Real meat and plant-based meat analogues have different in vitro protein digestibility properties. *Food Chemistry, 387*. https://doi.org/10.1016/j.foodchem.2022.132917

Young, P. M., Edge, S., Staniforth, J. N., Steele, D. F., & Price, R. (2005). Dynamic vapor sorption properties of sodium starch glycolate disintegrants. *Pharmaceutical Development and Technology, 10*(2), 249–259. https://doi.org/10.1081/pdt-54448

Zhang, K., Tian, X., Shen, R., Zhao, K., Wang, Y., Zhang, Y., et al. (2023). Delaying in vitro gastric digestion of myofibrillar protein gel using carboxymethylated cellulose nanofibrils: Forming a compact and uniform microstructure. *Food Hydrocolloids, 140*. https://doi.org/10.1016/j.foodhyd.2023.108661

Zhao, J., Wu, J., Chen, Y., Zhao, M., & Sun, W. (2020). Gel properties of soy protein isolate modified by lipoxygenase-catalyzed linoleic acid oxidation and their influence on pepsin diffusion and in vitro gastric digestion. *Cite This: Journal of Agricultural and Food Chemistry, 68*, 5698. https://doi.org/10.1021/acs.jafc.0c00808

Zuo, D., Chen, Y., Li, Y., Huang, X., Wang, Q., Wang, Y., et al. (2024). Cellulose as filler particle affects the poroviscoelasticity behavior of meat gels: Hydration properties and microstructure. *Food Hydrocolloids, 159*. https://doi.org/10.1016/j.foodhyd.2024.110620